Supplemental Figure Legends:

Supplemental Figure 1: Mutation of the identified D-, O- and A-boxes did not affect Claspin destruction by Cdh1.

(A) Sequence alignment of Claspin and other known Cdh1 substrates shows that the Claspin protein contains a canonical Destruction Box that could be recognized by the APC/Cdh1 E3 ligase complex.

(B) Illustration of the location of various potential D-, A- and O-boxes identified in the Claspin protein sequence, and the generated 3M/4M/5M Claspin mutants.

(C) Myc-Claspin and HA-Cdh1 or HA-Cdc20 constructs were co-transfected into HeLa cells as indicated, and the differences in Claspin expression levels were detected by anti-Myc immunoblot analysis.

(D) Immunoblot analysis of HeLa cells transfected with the indicated Myc-Claspin plasmid, synchronized by growth in nocodazole, and then released for the indicated periods of time.

Supplemental Figure 2: Claspin contains a novel degron at its N-terminus that governs its destruction by Cdh1.

(A) Myc-Claspin and HA-Cdh1 constructs were co-transfected into HeLa cells as indicated, and the differences in Claspin expression levels were detected by anti-Myc immunoblot analysis.

(B) Autoradiograms showing recovery of ^{35}S-labeled Claspin protein bound to GST-Cdh1 fusion proteins (GST protein as negative control).

(C) Immunoblot analysis of HeLa cells transfected with the indicated Myc-Claspin plasmids, synchronized by growth in nocodazole, and then released for the indicated periods of time.

(D) Autoradiograms of ^{35}S-labeled Claspin after in vitro ubiquitination by anti-APC immunoprecipitation from HeLa cells supplemented with Cdh1 in the presence of ubiquitin.

(E) Autoradiograms showing recovery of ^{35}S-labeled Claspin protein bound to GST-Cdh1 fusion proteins (GST protein as negative control).

Supplemental Figure 3: Depletion of Cdh1 leads to activation of Chk-1 activity.

(A) Depletion of Cdh1 by siRNA treatments leads to a significant induction of Claspin protein and activation of the Chk1 pathway in asynchronized HeLa cells.

(B-D) Overexpression of Claspin in HeLa **(B)**, LNCap **(C)** and U2OS **(D)** cells leads to increased phosphorylation of Chk1.

(E) Ectopic expression of Claspin in HeLa cells resulted in increased BrdU incorporation.

(F) Ectopic expression of Claspin in U2OS cells resulted in premature activation of the Chk1 pathway in the early G1 phase.

Supplemental Figure 4: Depletion of Cdh1 by lentiviral shCdh1 infection resulted in growth retardation in U2OS cells and primary human fibroblasts with intact p53/Rb pathways, but no growth arrest in HeLa cells.

(A) HeLa cells were infected with the indicated lentiviral shRNA constructs. 24 hours post-infection, cells were selected with 1μg/ml puromycin to eliminate the non-infected cells. Cells were replated and cell numbers were counted at the indicated times.

(B) U2OS cells were infected with the indicated lentiviral shRNA constructs. 24 hours post-infection, cells were selected with 1μg/ml puromycin to eliminate the non-infected cells. Cells were replated and cell numbers were counted at the indicated times.

(C) HeLa or U2OS cells were infected with the indicated lentiviral shRNA constructs. 24 hours post-infection, cells were selected with 1μg/ml puromycin to eliminate the non-infected cells. Cell lysates were collected for immunoblot analysis with the indicated antibodies.

(D) Immunoblot analysis of HeLa cells infected with shGFP or shCdh1 lentiviral vector, synchronized by growth in nocodazole, and then released for the indicated periods of time.

(E) Depletion of Cdh1 in U2OS cells resulted in accumulation of cells in the S phase. U2OS cells were infected with the indicated lentiviral shRNA constructs. 24 hours post-infection, cells were selected with 1μg/ml puromycin to eliminate the non-infected cells. Cell cycle distribution was examined by FACS analysis.

(F) Primary human lung fibroblast cells were infected with the indicated lentiviral shRNA constructs. 24 hours post-infection, cells were selected with 1μg/ml puromycin to eliminate the non-infected cells. Cells were replated and cell numbers were counted at the indicated times.

Supplemental Figure 5: Overexpression of SV40 LT-antigen leads to induction of both p53 and E2F1, while depletion of Cdh1 results in elevated Claspin expression in primary human fibroblasts.

(A-B) Creation of SV40 LT-antigen overexpressing primary human lung (**A**) or foreskin fibroblast (**B**) cell lines. Primary human lung or foreskin fibroblast cells were infected with pBabe-Neo-LT-ag retroviral construct. 24 hours post-infection, cells were selected with 0.4μg/ml neomycin to eliminate the non-infected cells. Cell lysates were collected for immunoblot analysis with the indicated antibodies.

(C) Primary human lung fibroblast cells were infected with the indicated lentiviral shRNA constructs. 24 hours post-infection, cells were selected with 1μg/ml puromycin for 48 hours to eliminate the non-infected cells. Whole cell lysates were collected for immunoblot analysis using the indicated antibodies.

Supplemental Figure 6: Inactivation of both the p53 and Rb pathways by overexpression of LT-antigen partially blocked the premature senescence phenotype induced by depletion of Cdh1 in primary human foreskin fibroblasts.

(A-B) Primary human foreskin fibroblasts (FF) and SV40 LT-antigen expressing FF (FF/LT) cells were infected with the indicated shRNA lentiviral vectors. 24 hours post-infection, cells were selected with 1 μg/ml puromycin to eliminate the non-infected cells. Whole cell lysates were collected at the indicated times post-infection. Six days after puromycin selection, cells were fixed by 70%

ethanol and the cell cycle distribution was examined by FACS analysis (**A**). Meanwhile, cells were incubated with 1μg/μl BrdU and 100 μg/μl Uridine for six hours prior to being fixed with cold methanol and subjected to immunohistochemical analysis using anti-BrdU antibody (**B**).

(C) Quantification of the percentage of BrdU positive cells in (**B**).

(D) Immunoblot analysis of FF and FF/LT cells infected with the indicated shRNA lentiviral vectors. 24 hours post-infection, cells were selected with 1 μg/ml puromycin to eliminate the non-infected cells. Whole cell lysates were collected at the indicated times post-infection for immunoblot analysis using the indicated antibodies.

Supplemental Figure 7: Cdh1 interacts with the hypophosphorylated form of Rb.

(A-B) Autoradiograms showing recovery of ^{35}S-labeled E2F1 (**A**) or Rb (**B**) protein bound to GST-Cdh1 fusion proteins (GST protein as negative control). Where indicated, in vitro translated Rb protein was incubated with cyclinA/Cdk2 kinase (**B)** prior to the pull-down assays.

(C) Autoradiograms showing recovery of ^{35}S-labeled Rb protein bound to GST-E2F1 fusion proteins. Where indicated, in vitro translated Rb protein was incubated with cyclinA/Cdk2 kinase prior to the pull-down assays.

(D) 293T cells were transiently transfected with various constructs as indicated. 48 hours post-transfection, cell lysates were recovered and Flag-immunoprecipitation was performed. The immunoprecipitates were denatured in SDS-containing sample

buffer and separated by SDS-PAGE before immunoblot analysis with the indicated antibodies.

Supplemental Figure 8: The C-box motif is required for Cdh1 to interact with Rb and for Cdh1 to induce E2F1 expression.

(A) Illustration of the ΔC-box and ΔIR-box Cdh1 mutants.

(B) The ΔC-box Cdh1 mutant is defective in Rb interaction. 293T cells were transiently transfected with various constructs as indicated. 48 hours post-transfection, cell lysates were recovered and HA-immunoprecipitation was performed. The immunoprecipitates were denatured in SDS-containing sample buffer and separated by SDS-PAGE before immunoblot analysis with the indicated antibodies.

(C) Ectopic expression of wild-type, but not the ΔC-box mutant Cdh1, leads to induced E2F1 expression in U2OS cells.

Supplemental Figure 9: Inactivation of Skp2 results in elevated E2F1 expression in HeLa cells.

Depletion of Skp2 by siRNA treatments leads to a significant induction of the E2F1 protein in asynchronized HeLa cells.

Supplemental Figure 10: dE2F1 protein levels are reduced in *fzr* mutant tissue of the eye disc.

(A) Mosaic clones of a *fzr*-null allele, fzr^{ie28}, were generated in eye discs using ey-FLP and FRT– fzr^{ie28}. fzr^{ie28} mutant clones are marked by the lack of green fluorescent protein (GFP) signal. Discs were immunostained with antibodies to GFP (green) and Cyclin B (red), respectively. The white arrows indicate the position of the morphogenetic furrow (MF). Anterior is to the left, posterior to the right. The white box in the right panel marks the area that is shown in higher magnification in (**B**).

(B) Higher magnification of an area within the eye disc. The white line the right panel marks clone borders.

(C-D) dE2F1 protein levels are reduced in *fzr* mutant tissue of the eye disc. (**C**) Mosaic clones of a *fzr*-null allele, fzr^{ie28}, were generated in eye discs using ey-FLP and FRT– fzr^{ie28}. fzr^{ie28} mutant clones are marked by the lack of green fluorescent protein (GFP) signal. Discs were immunostained with antibodies to GFP (green) and dE2F1 (red), respectively. The white arrows indicate the position of the morphogenetic furrow (MF). Anterior is to the left, posterior to the right. The white box in the right panel marks the area that is shown in higher magnification in **D**.

(**D**) Higher magnification of an area within the eye disc. The white line the right panel marks clone borders. Note that dE2F1 protein levels are clearly reduced in *fzr* mutant tissue within MF, where dE2F1 levels are high in wildtype tissue. dE2F1 levels are also reduced in mutant tissue posterior to the furrow, although to a lesser extent.

A

```
Claspin              QKRQALFKLNDEDGFEEEEE
Skp2                 MHRKHLQEIPDQSGNYTTSF
Securin              ATRKALCTV-NRATEKSVKT
Cyclin B             TKRAALGDLQNRGISRPIAA
Destruction Box
consensus              RXXLXXXXN/D/E
```

B

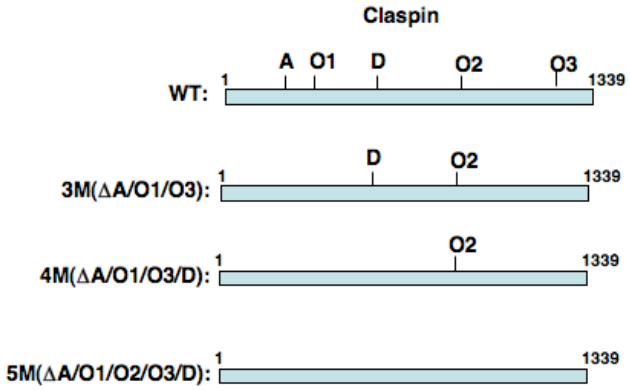

C

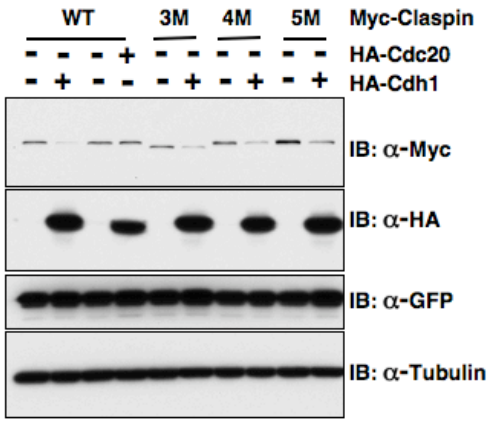

D

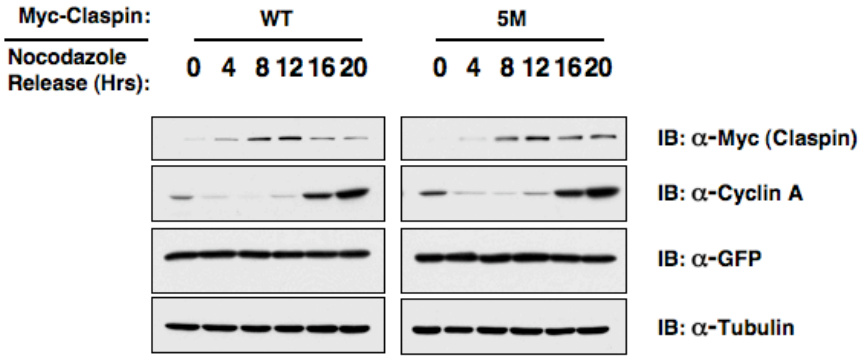

Supplemental Fig. 1

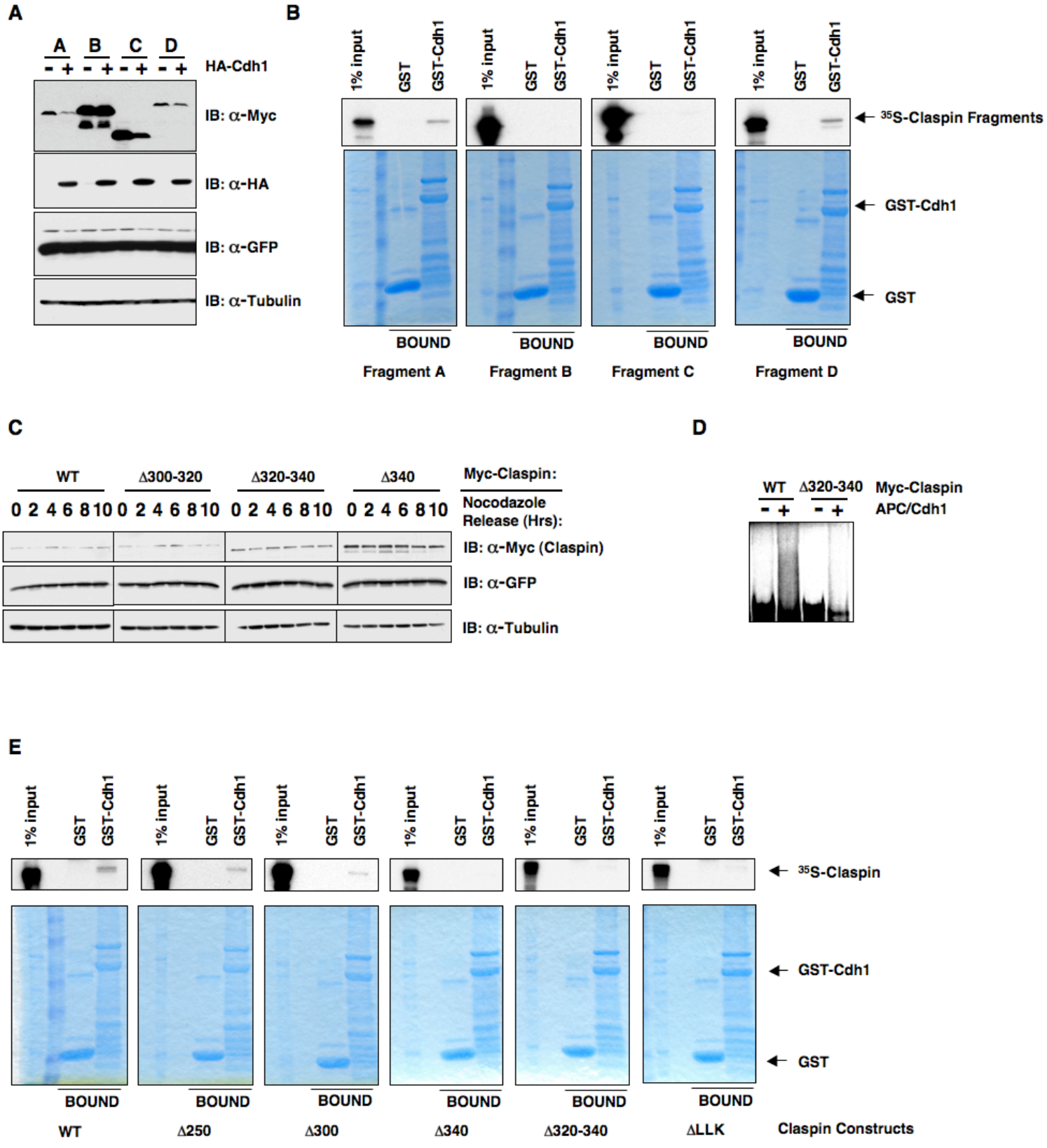

Supplemental Fig. 2

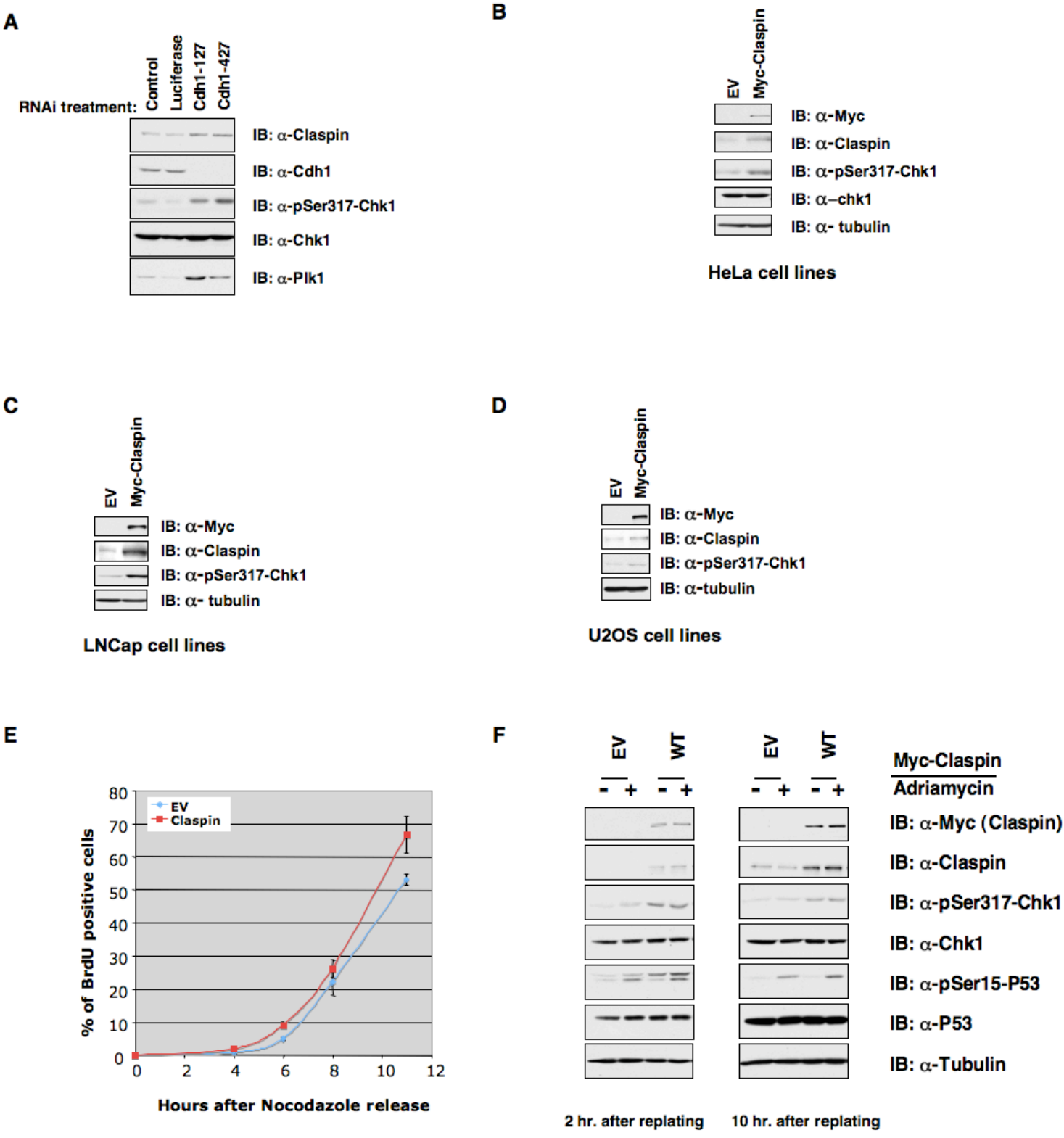

Supplemental Fig. 3

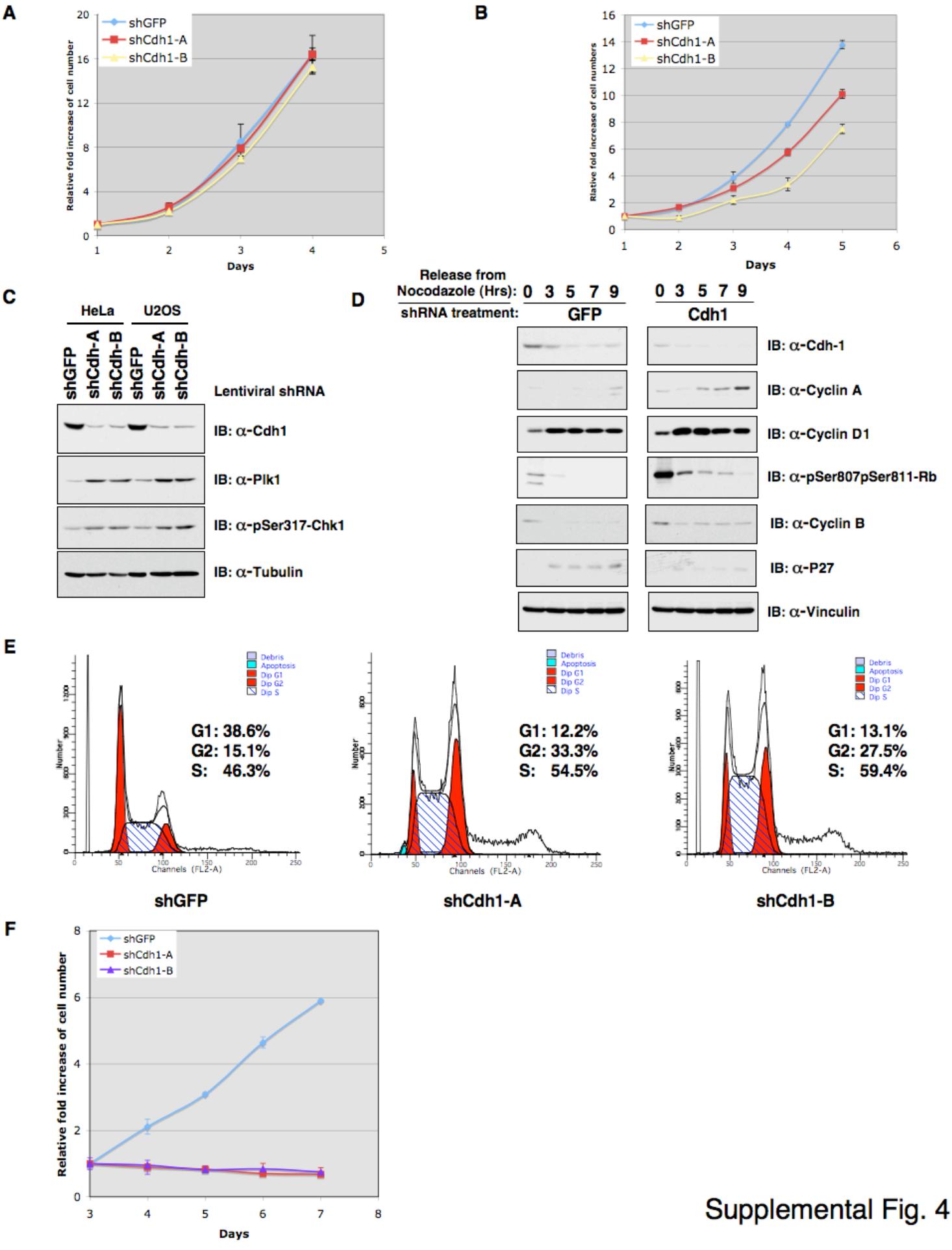

Supplemental Fig. 4

A

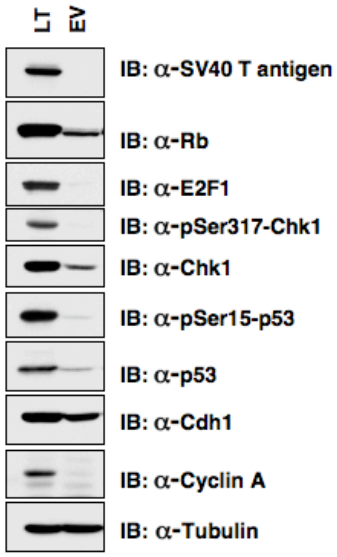

B

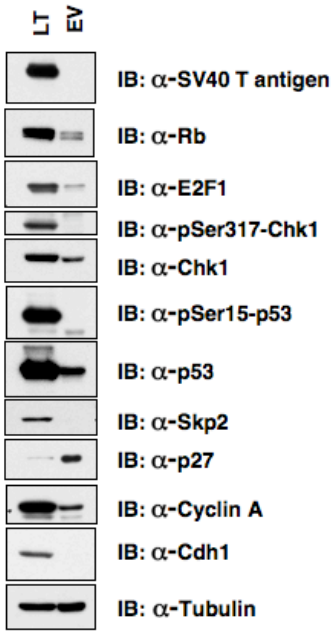

C

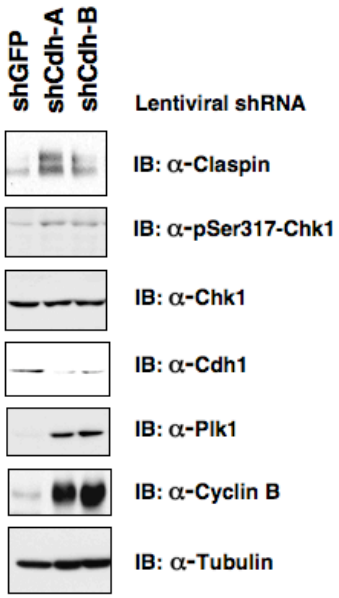

Supplemental Fig. 5

A

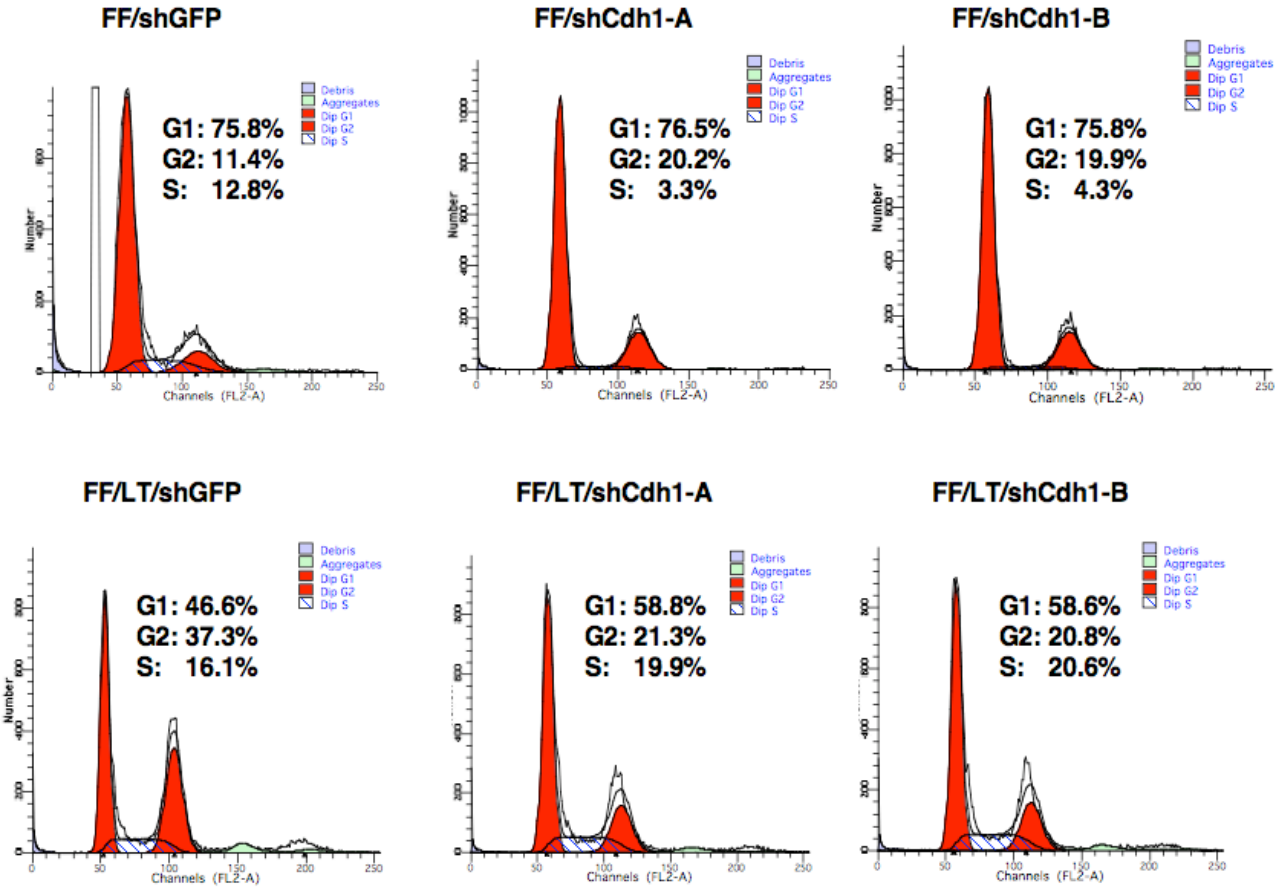

B

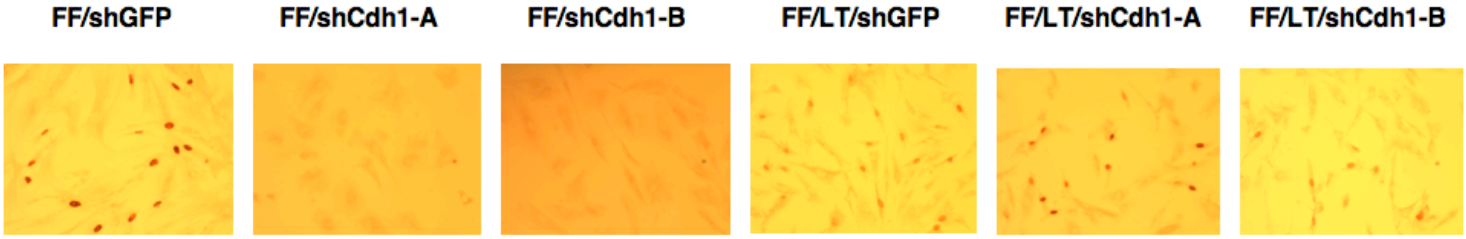

C

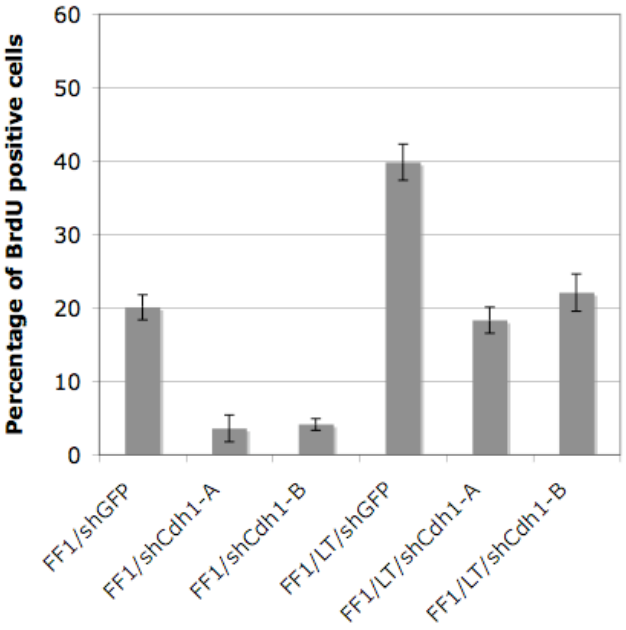

Supplemental Fig. 6

D

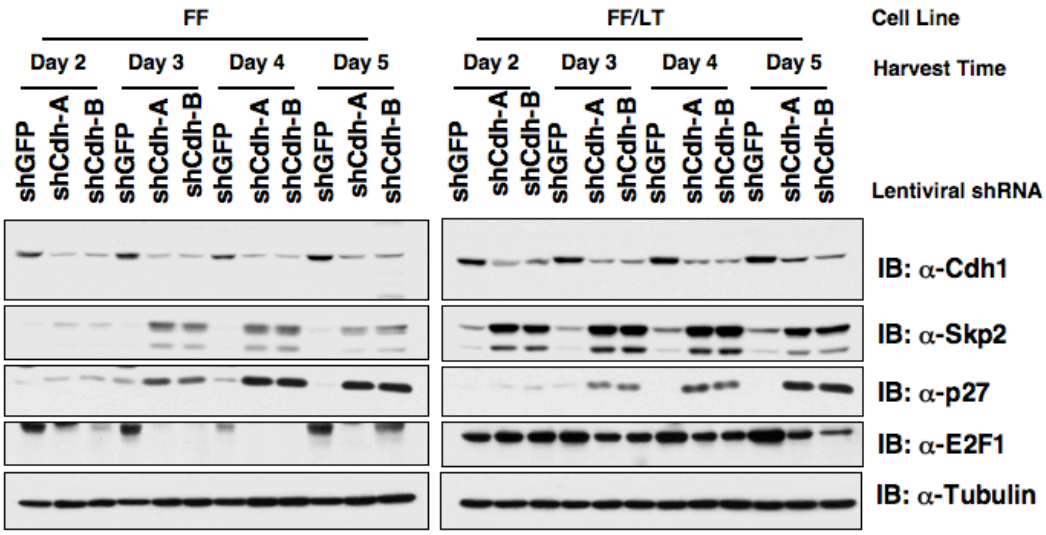

Supplemental Fig. 6

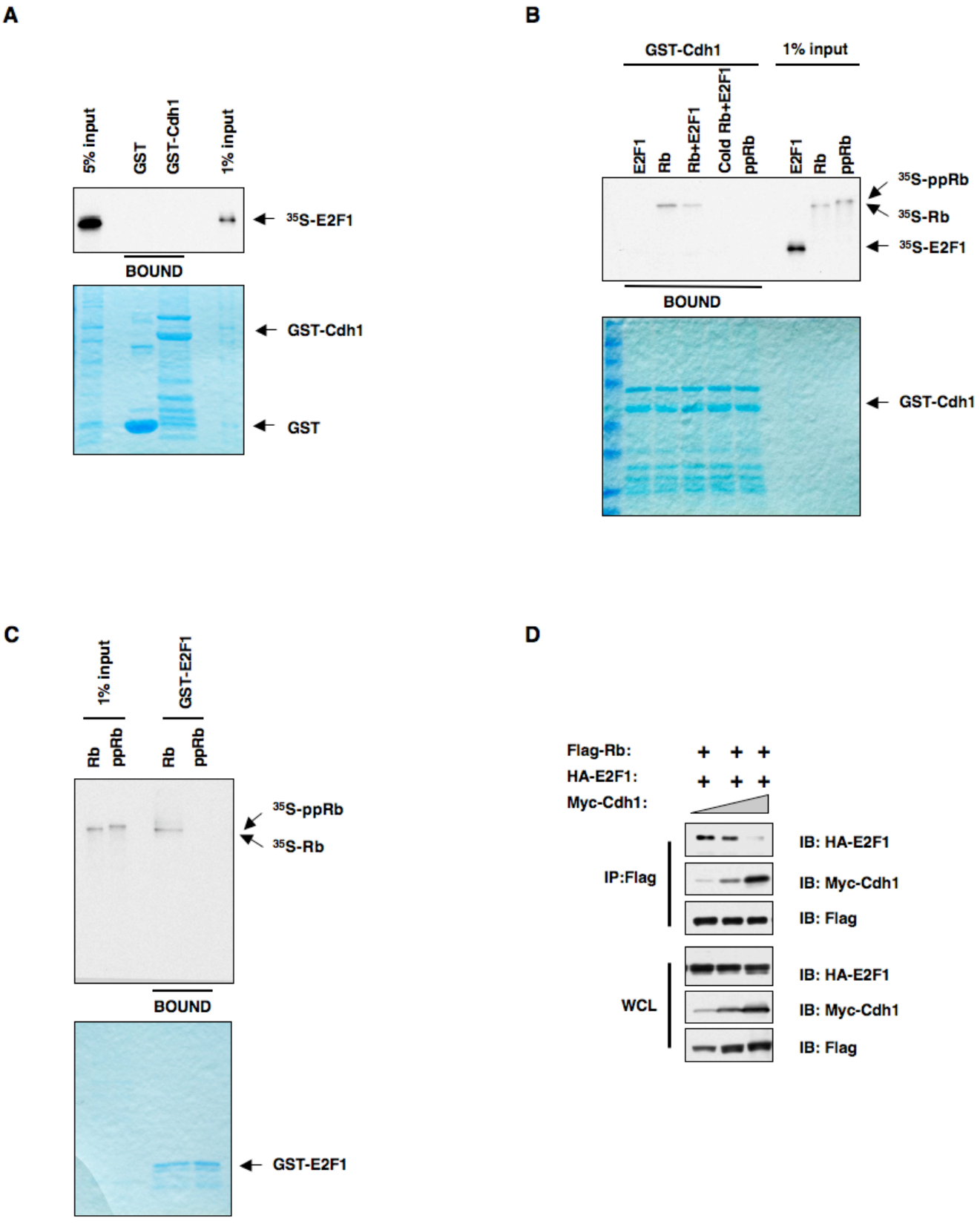

Supplemental Fig. 7

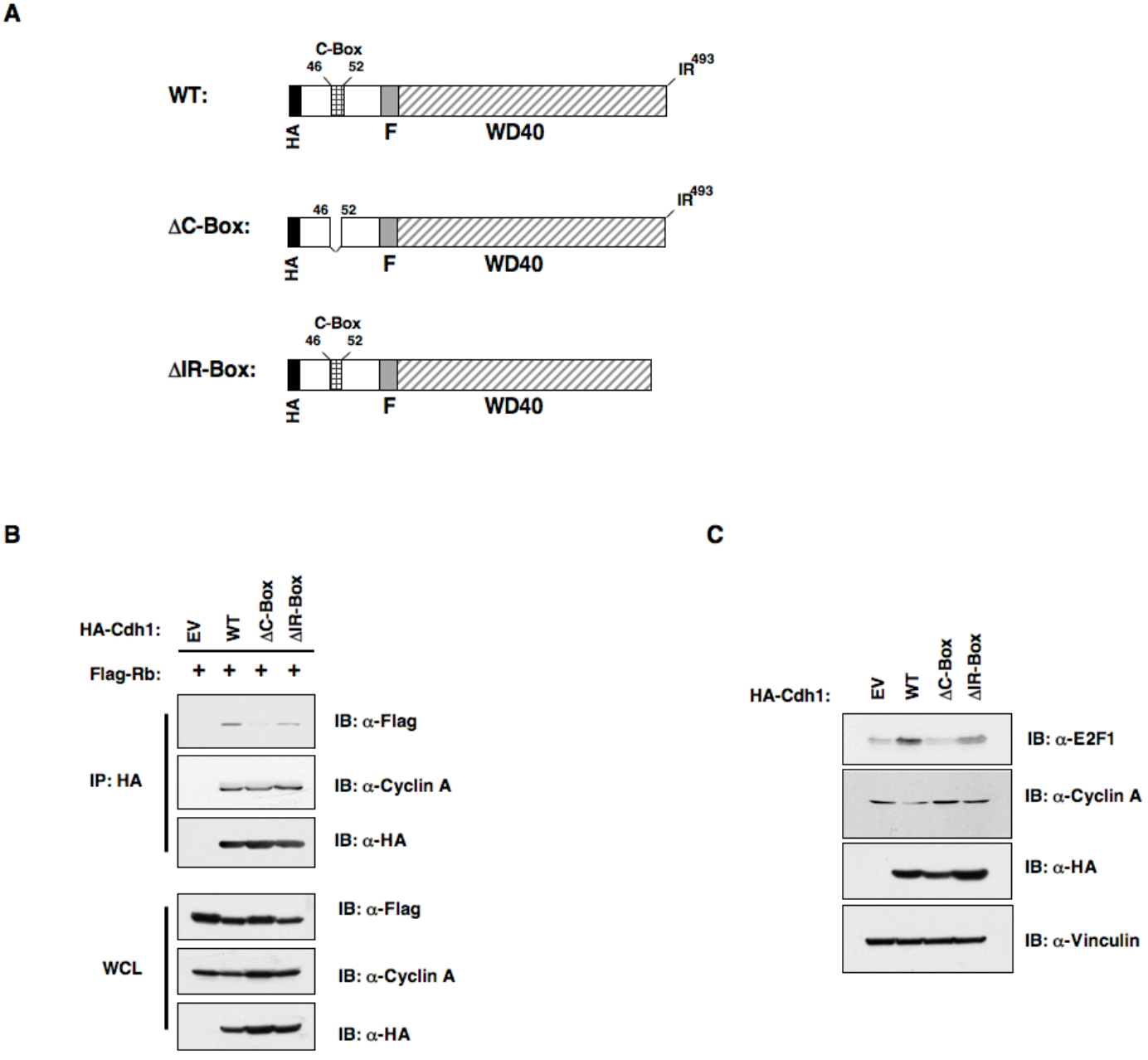

Supplemental Fig. 8

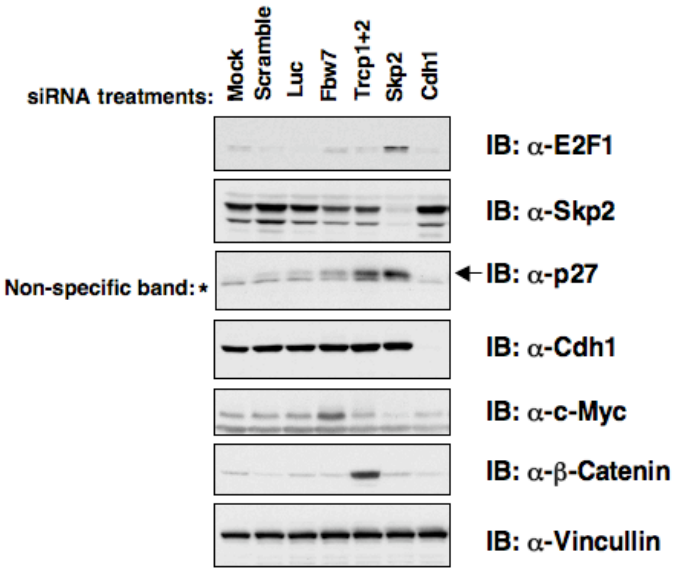

Supplemental Fig. 9

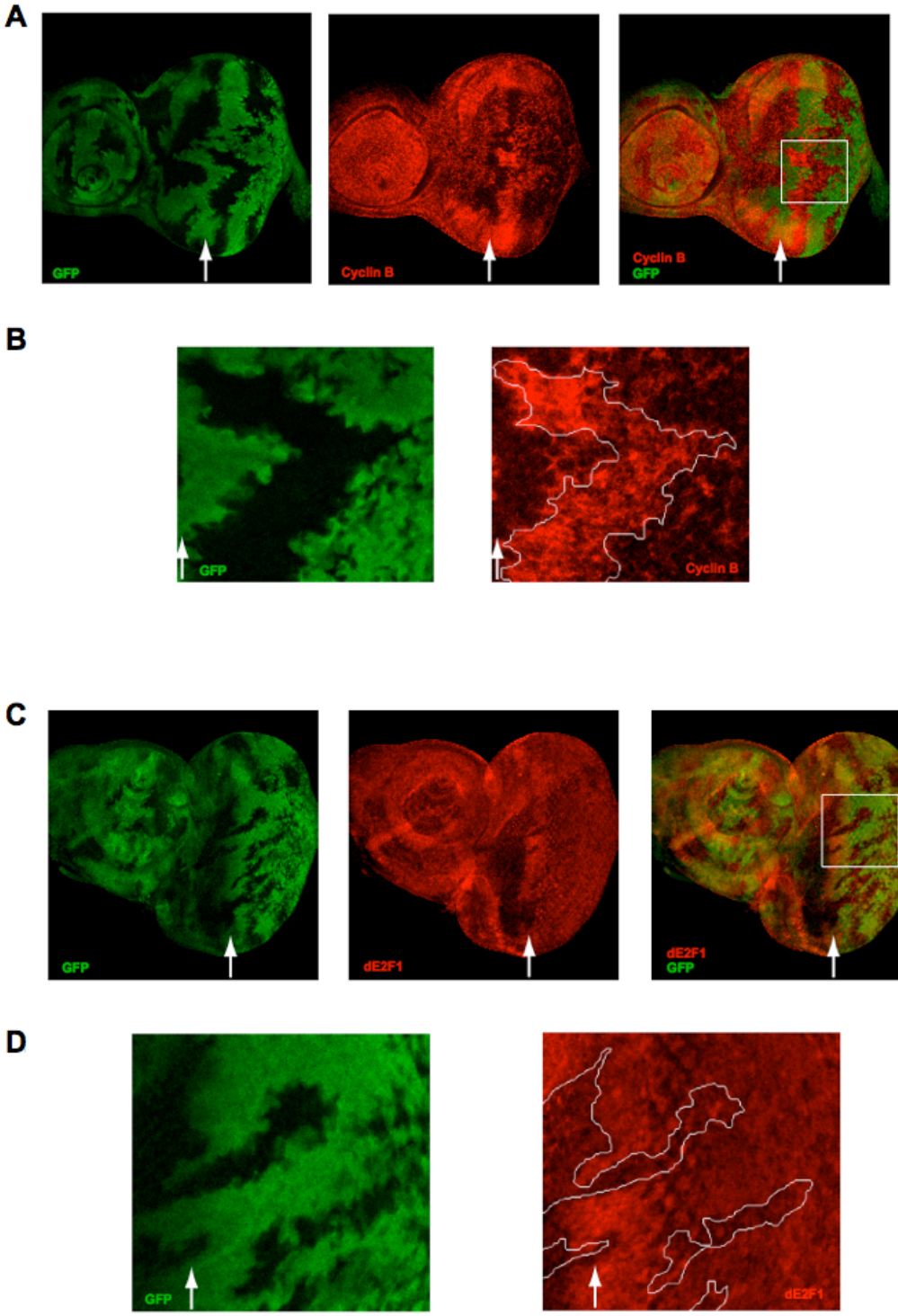

Supplemental Fig. 10